RASĀYAN *J. Chem.*
Vol. 18 | No. 1 |624-631| January - March | 2025
ISSN: 0974-1496 | e-ISSN: 0976-0083 | CODEN: RJCABP
http://www.rasayanjournal.com
http://www.rasayanjournal.co.in

POLYOLEFIN LITHIUM ION BATTERY (LIB) SEPARATOR TECHNOLOGY WITH ADDITION OF PVDF/NANO CHITOSAN COMPOSITE BLENDING MEMBRANE METHOD

T. Rihayat[1,✉], I. Mawardi[2], Usman[2], R. Munadi[4], M. Tadjuddin[4], D. Moentamaria[5], P.H. Suharti[5], J. Lianda[6], J. Custer[6], J. P. Siregar[7], A. Safitri[1], A. Ilmi[1] and A. Aida[1]

[1]Department of Chemical Engineering, Lhokseumawe State Polytechnic, Lhokseumawe-24301, Indonesia
[2]Department of Mechanical Engineering, Lhokseumawe State Polytechnic, Lhokseumawe-24301, Indonesia
[3]Department of Electrical Engineering, Syiah Kuala University, Banda Aceh- 23111, Indonesia
[4]Department of Mechanical Engineering, Syiah Kuala University, Banda Aceh- 23111, Indonesia
[5]Department of Chemical Engineering, Malang State Polytechnic, Malang-69323, Indonesia
[6]Department of Electrical Engineering, Bengkalis State Polytechnic, Bengkalis-28711, Indonesia
[7]Department of Materials Science and Engineering, Natural Fiber and Polymer Composites, Biocomposites, Universiti Malaysia Pahang, Pahang-26600, Malaysia
[8]Advanced Materials Engineering, Bandung Manufacturing Polytechnic
✉Corresponding Author: teukurihayat@yahoo.com

ABSTRACT

Separator is an important component in lithium ion batteries that is placed between the anode and cathode which functions to keep the two electrodes from touching directly and to prevent electrical short circuit. In addition, it is also a medium for transporting ions needed in the electrochemical process. This research aims to make a separator material with Polyolefin polymer with the addition of poly(vinylidene flouride) composite (PVDF/nano chitosan) using the membrane blending method. The comparison of PVDF/Nano chitosan composition variations are 10:0, 9:1, 8:2, and 7:3. The purpose of increasing the concentration fraction of nano chitosan to PVDF is to improve the performance of the composite separator, which includes porosity dimensions, pore density, and electrical conductivity. FTIR data shows that the material meets the criteria of composite materials, as the two phases can be distinguished by their molecular vibrational wave numbers. The higher concentration of nano chitosan resulted in a decrease in porosity dimension and an increase in porosity density, with the smallest pore dimension of 1.71 μm and pore density of 4.07x1011 count/m2 at a ratio of 7:3. This material can be categorized as a separator for lithium-ion batteries based on the above criteria.

Keywords: LIB Separator, Polyolefin, Nanochitosan, PVDF, and Blending Membrane Method.
RASĀYAN *J. Chem.*, Vol. 18, No.1, 2025

INTRODUCTION

Lithium-ion batteries play an important role as a power source in various portable electronic devices and hybrid and electric vehicles.[1] Lithium batteries are attractive to many users because they have high specific energy, high energy density, and longer usage time.[2] The separator is a porous membrane and is the most important part of the lithium-ion battery. The main function of the separator is to ensure ion flow and prevent short-circuiting.[3] An ideal separator has an ion resistance value of zero. A low ion resistance value can be obtained with a high porosity value.[2] The higher the porosity value, the lower the ion resistance value obtained.[1] Separators generally consist of a polymer membrane and form a microporous layer, which is a porous layer. The pore size of the separator is a critical factor, as it must be smaller than the particle size of the electrode components to function effectively. An ideal separator features uniformly distributed pores with a tortuous structure, which promotes uniform current distribution across the separator and helps inhibit lithium dendrite growth on the anode.

http://doi.org/10.31788/RJC.2025.1819079

Additionally, the porosity of the separator must be carefully optimized to facilitate efficient ion transport between the electrodes. The pore structure and the separator's ability to absorb electrolytes directly influence ionic conductivity. Separators with higher porosity can retain more liquid electrolytes, thereby enhancing the availability of ionic charge carriers for electrochemical processes. Balancing these properties is essential for optimal separator performance.[4] In addition, it improves the absorption of liquid electrolytes in the polymer matrix by controlling its components and morphology. Phase inversion is one of the main technologies in the manufacture of microporous membranes. According to Cui *et al*., The manufacture of PVDF membrane by the phase inversion method produces polymer electrolyte ion conductivity greater than 1 x 10-3 S/cm at room temperature.[5] Therefore, this method can be used in the manufacture of microporous membranes. Conventional separator materials in lithium-ion batteries, such as polyolefins—including polyethylene (PE) and polypropylene (PP)—are widely utilized due to their established properties. However, their low polarity results in limited liquid electrolyte absorption despite their high dielectric constant. This characteristic often leads to reduced ionic conductivity and a higher risk of electrolyte leakage. In contrast, semicrystalline polyvinylidene fluoride (PVDF) has garnered significant interest among researchers as a promising alternative for lithium-ion battery separators. Its high polarity and superior electrolyte absorption capacity make it an attractive candidate, potentially addressing the limitations associated with traditional polyolefin-based separators.[7] However, the disadvantage of the PVDF pore membrane is its high crystallinity.[8] To reduce the crystallinity of PVDF, two methods can be used: one is to combine the asymmetry group with the main chain of the polymer, and the other is to mix the polymer matrix (PVDF) with a suitable polymer or blending method.[9] The blending method is a simple method to modify the polymer matrix. Chitosan nanofiber can be explained due to the nature of the chitosan solution, which has high viscosity and surface tension.[10] The nature of the solution is influenced by the structure of D-glucosamine contained in chitosan, which has crystallinity and a high ability to hydrogen bond so that the chitosan solution is more like a cationic polyelectrolyte.[11] A solution with a high concentration and low viscosity makes it difficult to make nanofibers through the electrospinning process, so this research will use the spin coating method. By measuring morphology, phase analysis, functional group bonding, conductivity, resistance, etc., the effect of nano chitosan on PVDF membrane structure with variation of PVDF/Nano chitosan composition will be further investigated.

EXPERIMENTAL

Material and Methods

The materials used in this research are polyvinylidene fluoride (PVDF), nano chitosan, dimethylacetamide (DMAc), polyolefin, and distilled water. This section will describe the preparation and manufacturing process of membrane separators from polyolefin, nano-chitosan, and PVDF/Nano chitosan, as well as characteristic testing using FTIR, SEM, and TGA.

General Procedure

Separator Manufacturing Procedure

Synthesis PVDF/Nano chitosan

PVDF to be used as the main material for the manufacture of lithium ion battery separator was dissolved in N, N - dimethyl acetamide (DMAc) and added glycerol and Nano chitosan rotated for 6 hours at 700oC to homogenize the solution. The solution was spin-coated with an ITO glass substrate to form a thin layer. Before dispin coating, the ITO glass was first cleaned with an ultrasonic cleaner for 10 minutes and dried with tissue paper or optical tissue. After evaporation for 10 seconds, the thin layer is soaked in distilled water for 48 hours, and a porous membrane is formed. The purpose of this process is to remove glycerol, solvents, and additives. The soaked, thin film was dried under a vacuum at 400°C for 24 hours. PVDF/Nano chitosan porous membrane was formed.

Manufacture of Polypropylene Separator Modified with PVDF/Nano Chitosan Membrane

The first step was to prepare 21 ml of DMAc, 2.8 grams of PVDF, and 0.7 grams of Nano Chitosan. After that, 21 ml of DMAc with 2.8 grams of PVDF was stirred for 30 minutes, dissolved PP (Polypropylene) and PE (Polyethylene) using distilled water, then added 0.7 grams of Nano Chitosan stirred for 24 hours at 70ºC. After all materials were stirred, ultrasonication was carried out for 30 minutes at 30ºC, then

allowed to stand for 12 hours. Next, the spin coating process was carried out at a speed of 827 rpm to obtain a thin sheet sample. After that, it was soaked in a mixture of distilled water and DMAc for 30 seconds and then soaked with distilled water for 2 days, then oven for 12 hours at 60ºC. The PVDF/Nano chitosan samples were then characterized by FTIR, SEM, and TGA testing. Mechanical properties test: Tensile test and current density.

Detection Method

FTIR Spectroscopy

Infrared (IR) spectroscopy is a widely employed spectroscopic technique for analyzing polymeric materials. It encompasses two primary instrumental approaches: the dispersive method, which utilizes a prism or grating to disperse infrared radiation, and the Fourier transform (FT) method, which operates on the principles of interferometry (Malcolm, 2007). The fundamental principle of IR spectroscopy involves the absorption of infrared radiation by a compound, enabling the characterization of molecular vibrational states. By examining the intensity and spectral position (wavelength) of the absorbed infrared radiation, the elemental composition of the material under investigation can be determined. At a microscopic level, the material absorbs infrared radiation, which increases the vibrational amplitude of the bonded atoms, elevating the material to an excited vibrational state. When the molecule returns to its ground state, the absorbed energy is dissipated as heat. The specific wavelength absorbed is contingent on the type of vibrational motion occurring within the bonded atoms, resulting in distinct absorption values for different chemical bonds. The most commonly utilized range for infrared radiation in this technique lies between 4000 and 690 cm^{-1}, providing a robust framework for identifying and characterizing molecular structures. FTIR Spectroscopy testing was carried out at the Lhokseumawe State Polytechnic Chemical Engineering Laboratory in the wavelength range of 500 - 4000 cm^{-1}.

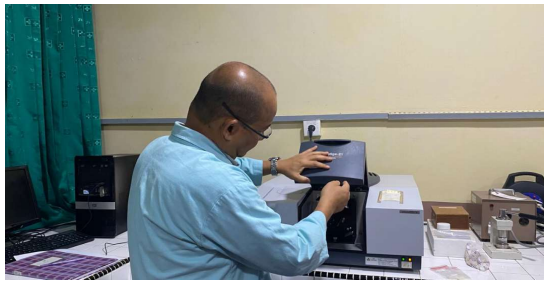

Fig.-1: Set of FTIR Spectroscopy Test Equipment

Scanning Electron Microscope (SEM) Test

Scanning electron microscopy (SEM) was employed to examine the surface morphology and layer thickness of the PVDF/Nano Chitosan separator. SEM is an advanced electron microscopy technique that generates high-resolution surface images of solid specimens by scanning them with a focused beam of high-energy electrons in a raster pattern. This method relies on the interaction of electrons with the atomic structure of the sample, producing various signals that convey detailed information about the sample's surface topography and compositional characteristics. During SEM imaging, the surface of the sample is bombarded with an electron beam, resulting in the emission of secondary electrons or backscattered electrons. These emitted electrons are captured by detectors, amplified, and subsequently translated into grayscale images displayed on a cathode ray tube (CRT) monitor. The contrast in these images, represented by variations in brightness, corresponds to the surface features of the sample. The secondary electron detector, a standard component in all SEM instruments, is capable of producing exceptionally high-resolution images, enabling the visualization of surface details at a scale of less than 1-5 nm. This allows for precise analysis of the sample's surface structure and morphology. A significant advantage of SEM is its ability to analyze samples without the need for thinning, thereby preserving their three-dimensional integrity. This feature makes SEM an invaluable tool for obtaining detailed, three-dimensional insights into the structural and morphological properties of materials.

Based on the SEM test results, the morphology of the pore structure of each PVDF/Nano Chitosan composition ratio and layer thickness will be obtained. From the SEM test results, the number of pores and pore density can be calculated using the following equation.

Fig.-2: SEM Test Equipment Set

TGA Thermogravimetric Analysis (TGA)

Thermogravimetric analysis (TGA) was conducted using a Shimadzu DTG-60 instrument to investigate the mass variation of the sample as a function of temperature, time, and atmospheric conditions. This technique operates on the principle of measuring the mass loss of a material as it is subjected to a controlled temperature increase, typically ranging from ambient temperature to approximately 800°C, at a constant heating rate of 20°C/min.[30] The analysis involves progressively raising the sample temperature while monitoring the corresponding mass changes, thereby providing insights into the thermal stability and decomposition behavior of the material. All specimens were analyzed under a continuous flow of nitrogen gas to maintain an inert environment and prevent oxidative degradation during the measurement process.

Fig.-3: A Set of TGA Test Equipment

RESULTS AND DISCUSSION

Analysis of FT-IR Spectroscopy Test Results

The bonding of functional groups in a compound in organic or inorganic materials can be identified using one of the spectroscopic tools, namely Fourier Transform Infrared (FTIR). FTIR is used to identify the type of chemical bond and polymer structure of the PVDF/Nano Chitosan composite separator, as shown in Fig.-4. The infrared spectrum of this material is highly dependent on its composition and the interaction between its main elements. The interaction simultaneously produces vibrational changes of atoms or molecules in the material that cause changes in the chemical and physical properties of the main elements (M. Usha Rani *et al.*, 2013). This FTIR test was carried out on the four samples, one sample in the form of pure PVDF powder and four samples in the form of membranes, namely the PVDF / Nano Chitosan composite separator with a composition ratio of 10:0, 9:1, 8:2, and 7:3. The wavelengths that appeared in the FTIR spectroscopy test of the PVDF / Nano Chitosan separator were compared with the FTIR results of pure PVDF powder.

The FTIR spectrum of pure PVDF is shown in Fig.-4 in the 500-4000 cm-1 region. At wave number 2345.44 cm^{-1} is the CH2 functional group asymmetric vibration. The strongest bond occurs at wave number 1726.29 cm^{-1}, which is the CH2 wagging functional group. The CH2 rocking functional group is a strong infrared bond at a wavelength of 505.35 cm^{-1}. A more complete FTIR spectrum of PVDF is tabulated in the table below. The FTIR results of the PVDF spectra provide some structural information to distinguish between crystalline and amorphous forms.

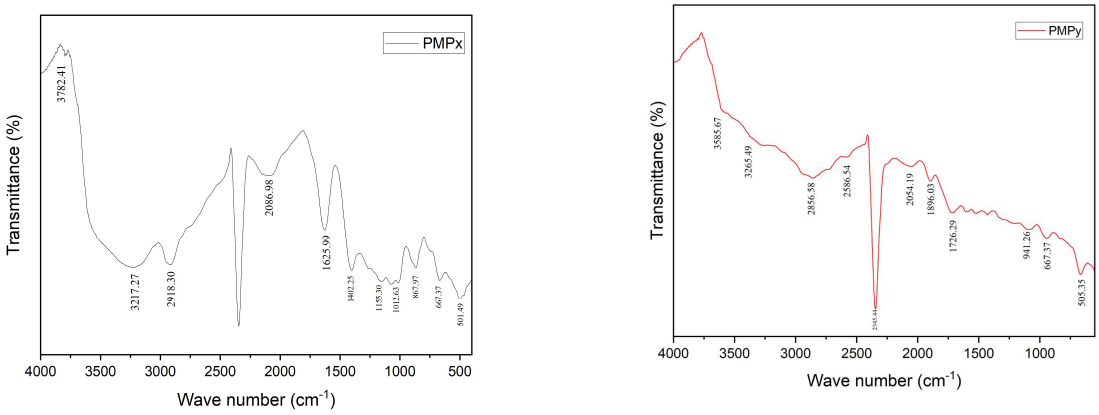

(a) (b)

Fig.4: Spectrum of PVDF/Nano Chitosan (PMP_x) and (PMP_y)

The functional group bonds in a compound, whether organic or inorganic, can be identified using one of the spectroscopic tools, namely Fourier Transform Infrared (FTIR) spectroscopy. FTIR is used to identify the types of chemical bonds and the polymer structure formed in the PVDF/PDMS composite separator, as shown in Fig.-4. The infrared spectrum of this material is highly dependent on its composition and the interactions among its main elements. These interactions simultaneously produce changes in the vibrations of atoms or molecules in the material, leading to alterations in the chemical and physical properties of the main components (M. Usha Rani *et al.,* 2013). FTIR testing was conducted on two samples: one sample consisted of pure PVDF powder, and the other was a membrane, specifically the PVDF/Nanochitosan composite separator with composition ratios of 10:0 and 7:3. The wave numbers obtained from the FTIR spectroscopy of the PVDF/Nanochitosan separator were compared with the FTIR results of the pure PVDF powder. The FTIR spectrum of the pure PVDF sample (PMPy) shows several characteristic absorption peaks that describe the structure and chemical composition of the polymer. Peaks at 3024 cm^{-1} and 2981 cm^{-1} correspond to the symmetric and asymmetric stretching vibrations of the CH_2 groups in the main chain of PVDF. The presence of these peaks indicates that the basic structure of the polymer remains intact. A sharp peak at 1403 cm^{-1} is characteristic of the bending vibration of CH_2 in PVDF. The strong intensity indicates the presence of a significant number of methylene groups in the polymer structure. The peak at 1180 cm^{-1} can be attributed to the symmetric stretching vibration of the CF_2 group. This is one of the main characteristic peaks of PVDF, indicating the presence of C-F bonds in the polymer structure. The peak at 841 cm^{-1} is particularly important as it relates to the β phase of PVDF, which is known for its excellent piezoelectric and electroactive properties, essential for lithium-ion battery separator applications. The presence of this peak indicates that the PVDF sample has a significant β phase component. The peak at 764 cm^{-1} is typically associated with the α phase of PVDF. Its presence alongside the β phase peak indicates that the PVDF sample has a mixed structure of both α and β phases. The range of peaks between 1000-650 cm^{-1} includes several peaks (such as at 764 cm^{-1}, 841 cm^{-1}, and 976 cm^{-1}) that collectively represent various vibrational modes of the PVDF main chain, including wagging and rocking vibrations of CF_2 and CH_2.

Analysis of Scanning Electron Microscope (SEM) Test Results

To qualitatively identify the morphology of the PVDF/Nano Chitosan composite separator, a SEM (Scanning Electron Microscope) can be used. The purpose of SEM testing is to determine the microstructure profile, layer thickness, and pore size of the PVDF/Nano Chitosan composite separator.

Based on Fig.-5 is the result of testing using Scanning Electron Microscopy (SEM) in the treatment of 500x magnification distance on PVDF /Nano Chitosan with a ratio of 10:0, 9:1, 8:2, and 7:3, it can be seen in the picture above that there are many clumps of samples that are widely spread due to electromagnetic beam. In the PVDF /Nano Chitosan sample, there are fewer sample blobs than the other samples; this shows that the morphology in each PVDF /Nano Chitosan comparison has a symmetrical pore structure.

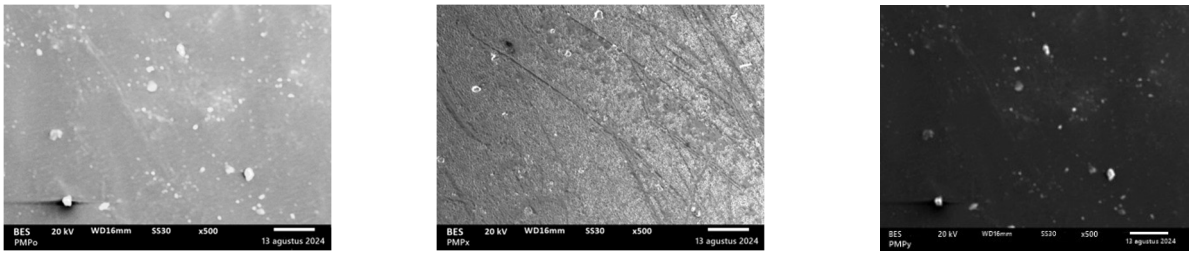

a b c

Fig.-5: SEM Test Results of Pore Separator With PVDF/Nano Chitosan Composition Ratio Comparison

The pore structure is formed due to the vacuum process for 24 hours. According to C.L. Cheng, the evaporation process in a vacuum can form a pore structure in the electrolyte separator (C.L. Cheng, 2004). At a ratio of 10:0, the geometry of the pore consists of two types, namely circles and ovals. Along with the addition of Nano Chitosan, the geometry of the pore shape tends to form a circle. SEM test Fig.-5 also shows the decreasing size with increasing concentration of Nano Chitosan in PVDF/Nano Chitosan composite separator. In the PVDF/Nano Chitosan comparison (10:0 or without Nano Chitosan) with the shrinking pore diameter, it shows that the number of pores from each comparison is increasing. This can be proven qualitatively and quantitatively, qualitatively as shown in the SEM test results in Fig.-5.

Analysis of TGA Test Results Thermogravimetric Analysis (TGA)

The process of mass loss in thermal tests occurs due to the decomposition process, namely the breaking of chemical bonds. Figure-6 is a graph of the TGA test results for Pure PVDF and PVDF/Nano Chitosan with the highest value in the previous test, namely the PVDF/Nano Chitosan (7:3) sample.

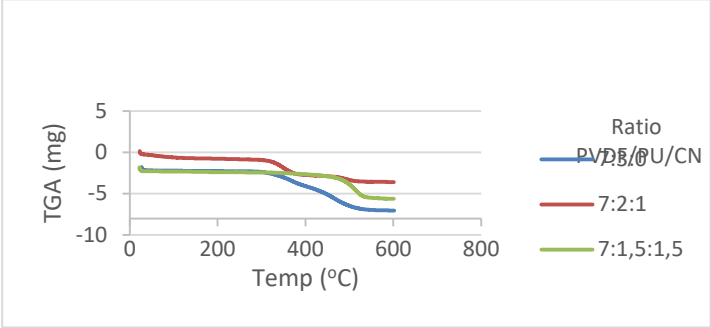

Fig.-6: PVDF/Nano Chitosan with a Ratio of 7:3 With Pure PVDF

The TGA test results characterize the changes in temperature and mass of the sample during heating. This test was conducted in an inert atmosphere using nitrogen gas to control thermal events such as melting, phase transitions, and decomposition. The PVDF/Nanochitosan separator was tested using TGA instrumentation to determine its thermal stability. The TGA results for PVDF/Nanochitosan are shown in Fig.-6. The onset of thermal degradation occurs at 359.74°C, indicating that the material has good thermal stability up to this temperature. The PVDF/Nanochitosan separator experiences three stages of decomposition, with midpoint data at 425.72°C and endset at 505.04°C, demonstrating that the decomposition process occurs over a wide temperature range. The first stage involves the evaporation of water and solvents, occurring from the initial temperature up to around 250°C. During this stage, bound water and residual solvents evaporate, resulting in a slight weight loss observed in the TGA curve. The second stage, with onset at 359.74°C, midpoint at 425.72°C, and endset at 505.04°C, involves the thermal decomposition of the polymer components. PVDF begins to decompose, releasing HF and forming double bonds. Nanochitosan also starts to decompose within this range. The final stage occurs above 505.04°C, where carbonization of the polymer residue takes place, along with further degradation of the remaining carbon structure. The total weight loss recorded was 4.684 mg (160.154%). This high percentage may indicate calibration or calculation errors, as weight loss should not exceed 100%. The graph shows the presence of residue after heating, which could originate from nanochitosan or interactions between PVDF and chitosan.

CONCLUSION

From the Findings of This Study, the Following Conclusions Can be Drawn

The blending method successfully facilitated the formation of a PVDF/Nano Chitosan composite separator with micro-scale features, achieving a minimum pore size of 1.71 μm at a 7:3 ratio. Increasing the PDMS concentration was observed to reduce the pore size of the separator, as evidenced by the high pore density of $4.07 \times 10^{11}/m^2$ attained at the 7:3 ratio. Additionally, this ratio exhibited a crystallinity degree of 29.26%. The incorporation of a higher concentration fraction of nano chitosan relative to PVDF aimed to enhance the composite separator's performance, particularly in terms of porosity, pore density, and electrical conductivity. FTIR analysis confirmed the composite nature of the material, as the distinct molecular vibrational wave numbers of each constituent phase remained identifiable, satisfying the criteria for composite materials. Given these characteristics, the developed material meets the essential requirements for use as a separator in lithium-ion batteries, demonstrating its potential for application in energy storage systems.

ACKNOWLEDGMENTS

The author expresses his sincere gratitude and appreciation to the Ministry of Research, Technology, and Higher Education of the Republic of Indonesia and Politeknik Negeri Lhokseumawe for funding through grant number 130/SPK/D.D4/PPK.01.APTV/IV/2024

CONFLICT OF INTERESTS

In this article, the authors declare that there is no conflict of interest related to the research conducted or the publication of the results of this study. All data and information presented are independent and not influenced by the interests of any third party. The authors guarantee that the entire research process was conducted objectively and in accordance with applicable ethical standards.

AUTHOR CONTRIBUTIONS

All the authors contributed significantly to this manuscript, participated in reviewing/editing and approved the final draft for publication. The research profile of the authors can be verified from their ORCID ids, given below:

Teuku Rihayat https://orcid.org/0000-0001-5943-8574
Januar Parlaungan Siregar https://orcid.org/0000-0002-8130-1168
Profiyanti Hermien Suharti https://orcid.org/0000-0002-1978-6475
Johny Custer https://orcid.org/0009-0003-3212-9845
Jefri Lianda https://orcid.org/0000-0002-7185-9395
Aida Safitri https://orcid.org/0000-0003-4724-6043
Atiqah Aida https://orcid.org/0009-0008-9896-9448

REFERENCES

1. D. Amru, A. Widi, R. M. Fika, P. Hendra, H. S. Lukmanul, *Journal of Electroanalytical Chemistry,* **952(117984)**, 1(2024), https://doi.org/10.1016/j.jelechem.2023.117984
2. C. Chuyun, L. Hangzhong, O. Chuying, H. Naigen, Z. Guojun, H. Haoqing, *Composites Communications*, **33(101217)**, 1(2022), https://doi.org/10.1016/j.coco.2022.101217
3. D. Zhou, D. Shanmukaraj, A. Tkacheva, M. Armand, G. Wang, Chem, **5(9)**, 2326(2019), https://doi.org/10.1016/j.chempr.2019.05.009
4. Z. Gaolong, J. Xiaopeng, C. Dongjiang, H. Weidong, *IJO Hydrogen Energy*, **45**, 2917(2020), https://doi.org/10.1016/j.ijhydene.2019.11.125
5. Gregory Chatel, Liudmila Novikova, Sabine Petit, *Applied Clay Science*, **119(2)**, 193(2020), https://doi.org/10.1016/j.clay.2015.10.019

6. I. Yusuf, M. Yunus, T. Rihayat, S. Yasara, N. Aidy, *Jurnal Polimesin*, **21(3)**, (2023), http://dx.doi.org/10.30811/jpl.v21i3.3871
7. K. Bicy, A.B. Gueye, D. Rouxel, N. Kalarikkal, S. Thomas, *Surfaces and Interfaces,* **31**,101977(2022), https://doi.org/10.1016/j.surfin.2022.101977
8. M. R. Asghar, M. T. Anwar, T. Rasheed, A. Naveed, X. Yan, and J. Zhang, *IOP Conference Series Materials Science and Engineering*, **654(1)**, 012017(2019), https://doi.org/10.1088/1757-899X/654/1/012017
9. J. Wang, J. Shen, J. Shi, Y. Li, J. You, F. Bian, *Journal of Membrance Science,* **670**, 121359(2023), https://doi.org/10.1016/j.memsci.2023.121359
10. S. Yang, X. He, T. Hu, Y. He, S. Lv, Z. Ji, Z. Zhu, X. Fu, W. Yang, Y. Wang, A. Supertough, *Advanced Functional Materials,***33(45)**, 230472 (2023), https://doi.org/10.1002/adfm.202304727
11. G. S. Si, P. Santhoshkumar, J. W. Park, C. W. Ho, N. Shaji, H. K. Kim, M. Nanthagopal, C. W. Lee, *Ceramics International*, **47**, 33554(2021), https://doi.org/10.1016/j.ceramint.2021.08.264
12. T. Rihayat, S. Amroel, *Advanced Materials Research*, **647**, 701(2013), https://doi.org/10.4028/www.scientific.net/AMR.647.701
13. Suryani, H. Agusnar, B. Wirjosentono, T. Rihayat, Z. Salisah, *Journal of Physics: Conference Series*, **953**, 012015(2018), http://dx.doi.org/10.1088/1742-6596/953/1/012015
14. Yusuf, M. Yunus, T. Rihayat, S. Yasara, N. Aidy, *Jurnal Polimesin*, **21(3)**,(2023), http://dx.doi.org/10.30811/jpl.v21i3.3871
15. W. Zhang, M. Wang, H. Zhao, X. Liu, R. Liu, X. Xie, Y. Wu, *Journal of Applied Polymer Science,* **138(35)**, 50872(2021), https://doi.org/10.1002/app.50872

[RJC-9079/2024]